Received May 1999
Accepted July 1999

Heat removal of in-tube viscous flows to air with the assistance of arrays of plate fins

Part I: theoretical aspects involving 3-D, 2-D and 1-D models

Antonio Campo
College of Engineering, Idaho State University, Pocatello, Idaho, USA

Keywords *Fins, Heat transfer, Flow*

Abstract *A detailed comparative study of the heat transfer augmentation of in-tube flows accounting for an array of equally-spaced plate fins attached at the outer surface is undertaken. The aim of the paper is to critically examine the thermal response of this kind of finned tubes to three different mathematical models: a complete 3-D distributed model, a reduced 2-D distributed/lumped hybrid model and two largely simplified 1-D lumped models. For the three models tested, the computed results consistently demonstrate that the simplest 1-D lumped model, with embedded arithmetic spatial- and geometric spatial-means of the angular external convective coefficients provide dependable algebraic estimates of the actual heat transfer provided by the 3-D distributed model with its indispensable finite-difference solution. Further, an arithmetic mean of the maximum and minimum heat transfer supplied by the 1-D lumped model delivered results that match those computed with the 3-D distributed model. The most important steps of the mathematical derivations have been highlighted. A representative group of thermal performance diagrams is explained with the intent to assist engineers engaged in the thermal design of externally finned tubes of compact heat exchangers and HVAC devices.*

Nomenclature

$Bi(\theta)$ = local Biot number, $Rh_e(\theta)/k_i$
Bi = angular-mean of $Bi(\theta)$
c_p = specific isobaric heat capacity
D = tube diameter
g = acceleration of gravity
$h_e(\theta)$ = local external convective coefficient
$\overline{h}_e$ = angular-mean of $h_e(\theta)$
h_i = local internal convective coefficient
$\overline{h}_i$ = axial-mean of h_i
k = thermal conductivity
L = length of heat exchange region
L' = dimensionless L for laminar flow, L/RRe_iPr_i
L'' = dimensionless L for turbulent flow, L/R
$\dot{m}$ = mass flow rate
N = number of equally-spaced plate fins
Nu_e = local external Nusselt number, h_eD/k_e
$\overline{Nu}_e$ = angular-mean of Nu_e
Nu_i = local internal Nusselt number, h_iD/k_i
$\overline{Nu}_i$ = axial-mean of Nu_i

The author wishes to express his gratitude to the Organization of American States (OAS) for a visiting professorship at the Pontificia Universidade Catolica do Rio de Janeiro, Brazil. Also, the author would like to thank Prof. Angela O. Nieckele of the Mechanical Engineering Department of this university for helpful discussions.

International Journal of Numerical Methods for Heat & Fluid Flow, Vol. 10 No. 3, 2000, pp. 334-354.

Nu_{eq} = local equivalent Nusselt number, UD/k_i
$\overline{Nu}_{eq}$ = axial-mean of Nu_{eq}
p = height of plate fin
Pr = Prandtl number, $\mu c_p/k$
Q_t = total heat transfer
Q_{max} = maximum heat transfer
r = radial coordinate
R = tube radius
$Ra_{e,o}$ = modified Rayleigh number, $(g\beta_e/\nu_e^2)(T_o - T_\infty)D^3 \cdot Pr_e$
$Ra_{e,w}$ = local Rayleigh number, $(g\beta_e/\nu_e^2)(T_w - T_\infty)D^3 \cdot Pr_e$
Re_e = external Reynolds number, $\rho u_\infty D_e/\mu_e$
Re_i = internal Reynolds number, $4\dot{m}/\pi D\mu_i$
t = thickness of plate fin
T = temperature
<T> = angular mean of T
U = local, overall heat transfer coefficient
$\overline{U}$ = axial-mean of U
w = axial velocity
$\overline{w}$ = radial mean of w
x = coordinate along the circumference of the tube
X = dimensionless x
z = axial coordinate
Z = dimensionless z for laminar flow, z/RRe_iPr_i

Greek symbols
β = coefficient of thermal expansion
η = dimensionless r
θ = angular coordinate
μ = dynamic viscosity
ν = kinematic viscosity
ρ = density
ϕ = dimensionless T
Ω_t = dimensionless Qt

Subscripts
b = mean bulk
e = external fluid
i = internal fluid
f = finned segment
o = entrance
s = solid
u = unfinned segment
∞ = ambient

Introduction

The primary consideration associated with the design of heat exchanger tubes is the maximum rate at which heat transfer can be intensified actively or passively. Augmentation of forced convection heat transfer in tube flows may be achieved passively by fitting a uniformly-spaced array of radial or plate fins to the outer surface of circular tubes (see Bergles (1998) and Webb (1994)).

Because the external gas-side heat transfer coefficient is typically much smaller than the internal tube-side heat transfer coefficient, it is important to increase the gas-side Ah_e product. A primary surface geometry will increase the gas-side Ah_e product by simply increasing the area A. Since the gas-side heat transfer coefficient may be 5 to 20 per cent that of the tube-side heat transfer coefficient the use of closely spaced high fins is desirable. Fins for liquids normally use lower heights than that used for gases because liquids have higher heat transfer coefficients than gases.

From a fundamental standpoint, the problem on internal forced convection in externally finned tubes (annular and plate fins) is classified as a 2-D or a 3-D thermal entrance problem depending on the layout of the bundle of fins. Invariably, the local external convective coefficient, varies periodically along the tube for a layout of annular fins or along the periphery of the tube for a layout of axial plate fins. Consequently, both problems are subjected to a thermal boundary condition of third kind at the tube wall.

An analysis was carried out by Sparrow and Charmchi (1980) for the case of fully developed laminar flow in externally finned tubes having a regularly-spaced array of annular fins or square plates affixed to the outside surface of the tube. Finned tubes of this type abound in residential and institutional space heating systems. These authors formulated the thermal entrance problem with a 2-D distributed model that was controlled by a dominant thermal boundary condition in which the external heat transfer coefficient, $h_e(z)$, varied periodically along the flow direction. The periodic variation of $h_e(z)$ was idealized as a succession of high and low values, h_f and h_u, capable of modeling the successive finned and unfinned portions of the tube, z_f and z_u, respectively. An implicit finite-volume procedure was implemented to solve the dimensionless energy equation with a Poiseuillean velocity and a prescribed periodic boundary condition in terms of Bi. The computational task required to obtain the numerical solutions were especially demanding because of the abrupt periodic changes in Bi. The grid consisted of 220 points in the radial direction with a greater concentration of points near the tube wall. For the axial direction the uniform step sizes were of the order of 10^{-5} or 10^{-6} depending on the parameters, so that the number of points in the axial direction ranged from 50,000 to 95,000. Despite the fact that Schmidt (1963) and Legkiy *et al.* (1974) have reported experimental data for the external convection coefficients which could have been used as valuable input in Sparrow and Charmchi (1980), theoretical values were assigned to h_f and h_u ($h_f >> h_u$) and to z_f and z_u ($z_f << z_u$) in order to perform the numerical computations. With a view to finding a means to avoiding the lengthy computer intensive calculations for the periodic Biot numbers, an arithmetic-spatial-mean Biot number intended to approximate the heat transfer characteristics for the true periodic Biot number was proposed in Sparrow and Charmchi (1980). Certainly, this alternate approach provided adequate upper bounds for the actual mean bulk temperature distributions at low Biot numbers. Inexplicably, other spatial-mean Biot numbers, like the geometric-spatial-mean and the harmonic-spatial-mean Biot numbers that are linked to the equally important lower bounds for the actual mean bulk temperature distributions were not examined in this publication.

Moukalled *et al.* (1992) literally extended the work of Sparrow and Charmchi (1980) for the situation pertinent to turbulent flow employing the simple mixing length model. Likewise, these authors utilized an arithmetic-spatial-mean Biot number only to approximate the heat transfer characteristics for the true periodic Biot number of the fins, and no other spatial-mean Biot number was attempted.

From the perspective of engineering practice, Webb (1994) has stated that operational constraints, such as the gas-side fouling, may limit the annular fin density in externally finned tubes, like the arrays used in Sparrow and Charmchi (1980) and Moukalled *et al.* (1992). For instance, HVAC applications

employ 500-800 fins/meter, process air coolers are usually limited to 400 fins/meter, and applications involving dirty-soot-laden gases are restricted to 200 fins/meter.

The present paper addresses the other possible fin configuration that is connected to tubes covered with an array of axial plate fins. In contrast to the two-dimensional thermal entrance problem tackled in Sparrow and Charmchi (1980) and Moukalled *et al.* (1992), the nature of the present problem is indeed three-dimensional. It appears that the latter has not heretofore been addressed so far in the heat transfer literature. For each fin configuration, a minimum of four independent parameters need to be specified, namely: the "effective" convective coefficient for the finned segment, h_f, the fin thickness, x_f, the convective coefficient of the unfinned segment, h_u, and the interfin spacing, x_u, respectively.

In the absence of a viable analytical solution, a finite-volume technique has been employed. The numerical solutions are carried out through the entire thermal entrance region and were terminated when thermally developed conditions were attained. Further, to complement and provide perspective to the complete 3-D numerical results (the baseline solution), degraded 2-D and even a crude 1-D models relying on the ableness of a constant $\bar{h}_e$ (invariant with the angular coordinate, θ) were explored also. Clearly, adoption of a constant $\bar{h}_e$ necessitates a careful implementation of various spatial-means of the local, external convective coefficient, $h_e(\theta)$ within the framework of statistical analysis. In this regard, it should be added that the heat transfer literature relative to the applications of statistical aspects of spatial-means for the estimation of asymmetrical external convective coefficients arising in forced convection tube flows with bundles of fins is scarce. Therefore, an investigation focusing on the testing, validation and limitations of various spatial-means of $h_e(\theta)$ is necessary for purposes of exploring potential simplifications for the thermal design of externally finned tubes that are used in heat exchange devices. Correspondingly, the intent of this study is two-fold: first, to simulate realistically the heat transfer phenomenon itself with a complete 3-D distributed model; and second, to assess the relative importance of statistically-determined bounds utilizing two dependable lower-order models, such as a 2-D distributed/lumped hybrid model and a full 1-D lumped model.

In sum, the outcome of this comparative study may be relevant to:

- the general understanding of heat transfer behavior of flows inside externally finned tubes;
- the actual thermal design of finned tubes arising in heat exchange devices; and
- interactive engineering education in courses on design of thermal systems.

For the theoretical distributions of the axial-mean Nusselt numbers which are required for the models,see Appendix A.

Physical situation

It is well known that the addition of plate fins of thickness t and height p to the outer surface of circular tubes can be justified if the fin effectiveness ratio $(ht/k_s)^{1/2} << 1$ (see Mills, 1992). Under these premises, the inequality suggests the use of plate fins made from highly conducting metals for the natural convection heat removal to a gaseous medium such as air. Figure 1 depicts a circular tube fitted with an array of equally-spaced, external plate fins, together with the patented angular variation of the local external convective coefficient, $h_e(\theta)$, along the periphery of the tube.

The degree of heat transfer augmentation is sensitive to the number of equally-spaced fins in the array, N; the fin thickness, x_f; the "effective" convective coefficient for the finned segment, h_f, the unfinned segment, x_u, the convective coefficient of the unfinned segment, h_u; respectively. The thermal quantity of paramount importance for engineers involved in the design of finned tubes is the total heat removal, Q_t, that happen in a certain tube length, L. The heat losses from the internal fluid flow to the external air at a uniform

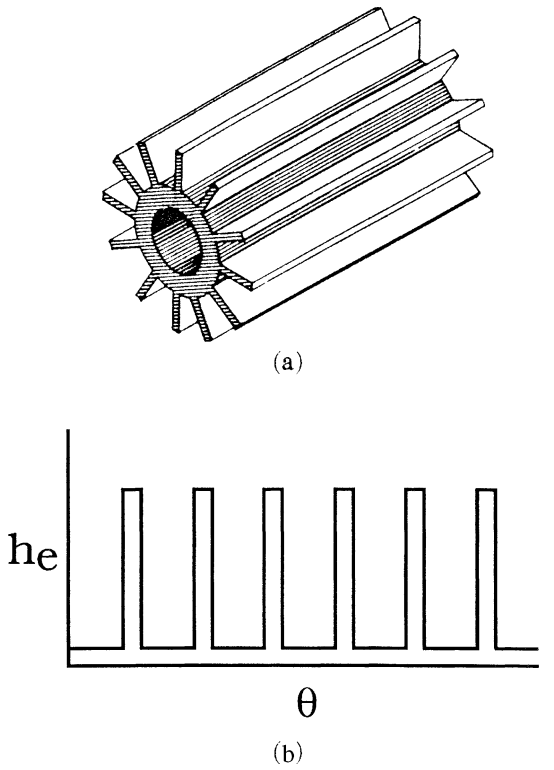

Figure 1.
(a) Sketch of the externally finned tube and (b) the angular variation of the local external convective coefficient

temperature, T_∞, occur through a sequence of unfinned and finned portions along the periphery of the tube. Jakob (1949) has advocated for the calculation of Q_t by way of a global energy balance between the inlet, z = 0, and a desired downstream station, z = L:

$$Q_t = rh\ c_{p,i}[T_o = T_b(L)] \tag{1}$$

Here, the mean bulk temperature, T_b, for incompressible viscous flows is computed from

$$T_b(z) = \frac{2}{R_2 u_m}\int_0^R u(r)T(z,r)\ rdr \tag{2}$$

where the specific heat capacity, c_p, has been assumed constant or averaged over the actual temperature interval of operation. Therefore, knowledge of T_b at any downstream station, L, is synonymous with the total heat transfer, Q_t, up to that station. This thermodynamic procedure avoids the calculation of an additional thermal quantity, the local distribution of the finned-tube Nusselt number Nu_z, which among other things, depends on the geometric and thermal characteristics of the fin array as well as the type of cooling.

First, attention has been confined to laminar motion. The velocity and temperature of an internal viscous fluid develop simultaneously from their respective uniform values, w_o and T_o, at the inlet of a heat exchange section, z = 0. According to Kays and Crawford (1993), this general situation for water, oil and other high-Prandtl number fluids ($Pr \geq 5$) can be modeled by a limiting situation in which the velocity is taken as fully developed and the temperature is developing.

Irrespective of the mathematical model adopted, the problem under study here is described by three dimensionless variables

$$\Phi = \frac{T - T_0}{T_\infty - T_0}, \quad Z = \frac{z}{R\ Re_i\ Pr_i}, \quad \eta = \frac{r}{R} \tag{3}$$

and four dimensionless parameters

$$N, \quad X_f = \frac{t}{D}, \quad Bi_u = \frac{Rh_u}{k_i}, \quad Bi_f = \frac{Rh_f}{k_i} \tag{4}$$

because N, X_f and X_u are interrelated through the tube perimeter.

3-D distributed model

Variable external convective coefficient: $h_e(\theta)$

Under the idealization that the properties of the internal fluid (water, oil or other high Pr fluid) are unaffected by temperature and ignoring heat conduction in the thin tube wall, the applicable 3-D energy conservation equation is given by

$$(1-\eta^2)\frac{\partial\Phi}{\partial Z}=\frac{1}{\eta}\frac{\partial}{\partial\eta}\left(\eta\frac{\partial\Phi}{\partial\eta}\right)+\frac{1}{\eta_2}\frac{\partial^2\Phi}{\partial\theta^2} \tag{5}$$

The imposed boundary conditions are written as

$$\Phi=0,\quad Z=0 \tag{6}$$

$$\frac{\partial\Phi}{\partial\eta}=0,\quad \eta=0 \tag{7}$$

$$-\frac{\partial\Phi}{\partial\eta}=Bi_f(\Phi-1),\quad \eta=1,\ 0<\theta<\beta_f \tag{8a}$$

$$-\frac{\partial\Phi}{\partial\eta}=Bi_u(\Phi-1),\quad \eta=1,\ \beta_f<\theta<\beta \tag{8b}$$

$$\frac{\partial\Phi}{\partial\theta}=0,\quad \theta=0,\ 2\pi;\quad all\ \eta \tag{9,10}$$

The preceding equations (5)-(10) have been solved numerically by the finite volume method of Patankar (1980), in which the physical domain was divided into contiguous curvilinear control volumes. Exploiting symmetry, the computational domain was reduced to a pie-shaped modulus, where the inequality $0 \leq \theta \leq \beta = \pi/N$ is susceptible to the number of fins, N. Of course, extra boundary conditions of lesser importance are needed at the symmetry lines, but they are omitted for brevity.

The resulting system of algebraic equations was solved by the line-by-line procedure of the tri-diagonal-matrix-algorithm (TDMA). The block correction algorithm suggested by Settari and Aziz (1973) was incorporated to enhance the convergence rates. Various nonuniform grids were constructed in the $\theta \times \eta$ computational domain where the grid lines were closely packed near the wall and also near the location of the fins. In addition, nonuniform axial steps ΔZ were smaller near the entrance (Z = 0), increasing in size gradually towards the less demanding downstream region. A sensitivity analysis of the grid reflected that a 22×36 nonuniform grid provided reasonable mean bulk temperature distributions (a global quantity) that were grid independent. For the limiting case ($N = 0$, $Bi_u = Bi_f = 1{,}000$), acceptable mean bulk temperature distributions have been obtained when compared with those accurately computed by Shah and London (1978) by exact techniques. An overall examination of the computations indicated that the results for the Nusselt number distribution are accurate to at least 0.1 percent.

2-D distributed/lumped hybrid model

Angular-mean external convective coefficient: $\bar{h}_e$

To simplify the 3-D distributed model and its unavoidable numerical calculations a lower order hybrid model inspired in a radially-distributed angularly-lumped structure could be sought. In principle, this simpler route, if successful, may relax the 3-D energy equation and more importantly simplify the convective boundary condition at the wall, Equations (8a) and (8b), markedly. This issue is analogous to the replacement of a periodic variation of Bi(θ) with some sort of a spatial-mean Biot number, $\bar{Bi}$, which is angular-independent.

Multiplying Equation (5) by $\eta^2 d\theta$ and later integrating between the limits 0 and 2π gives

$$\int_0^{2x} \eta^2(1-\eta^2)\frac{\partial \Phi}{\partial Z}d\theta = \int_0^{2x} \eta \frac{\partial}{\partial \eta}\left(\eta \frac{\partial \Phi}{\partial \eta}\right)d\theta + \int_0^{2x} \partial\left(\frac{\partial \Phi}{\partial \theta}\right) \tag{11}$$

In accordance with Leibniz rule (see Courant and Hilbert, 1953), the LHS and the first term of the RHS of Equation (11) are reordered to permit the derivative to occur before the integration. Because the upper and lower limits of the integrals are numbers, this operation yields

$$\eta^2(1-\eta^2)\frac{\partial}{\partial Z}\int_0^{2x} \Phi d\theta = \eta \frac{\partial}{\partial \eta}\left(\eta \frac{\partial}{\partial \eta}\int_0^{2x} \Phi d\theta\right) + \int_0^{2x} \partial\left(\frac{\partial \Phi}{\partial \theta}\right) \tag{12}$$

Owing to the definition of the angular mean temperature

$$\langle \Phi \rangle = \frac{1}{2\pi}\int_0^{2x} \Phi d\theta \tag{13}$$

Equation (12) may be converted into

$$\eta^2(1-\eta^2)\frac{\partial \langle \Phi \rangle}{\partial Z}2\pi = \eta \frac{\partial}{\partial \eta}\left(\eta \frac{\partial \langle \Phi \rangle}{\partial \eta}\right)2\pi + \left(\frac{\partial \Phi}{\partial \theta}\right)_{\theta=2x} - \left(\frac{\partial \Phi}{\partial \theta}\right)_{\theta=0} \tag{14}$$

Introduction of the angular boundary conditions of Equations (9) and (10) nullifies the second and third terms of the RHS of Equation (14) immediately. The end result is the 2-D energy equation

$$(1-\eta^2)\frac{\partial \langle \Phi \rangle}{\partial Z} = \frac{1}{\eta}\frac{\partial}{\partial \eta}\left(\eta \frac{\partial \langle \Phi \rangle}{\partial \eta}\right) \tag{15}$$

where the dependent variable is <Ú>. Now, in conformity with the two dimensionality of Equation (15) the discontinuous boundary conditions of Equations (8a) and (8b) need to be substituted by an equivalent boundary condition of third kind of continuous form written in terms of <Ú>. This action may be achieved by proposing a spatial-mean Biot number, $\overline{Bi}$, which fusions

Equations (8a) and (8b) into the following

$$-\frac{\partial\langle\Phi\rangle}{\partial\eta} = \overline{Bi}(\langle\Phi\rangle - 1), \quad \eta = 1 \tag{16}$$

The form of this equation stipulates a common boundary condition which controls the heat liberation through consecutive finned and unfinned segments around the tube. In this regard, three candidate spatial means for the Biot numbers are listed in Appendix B.

Equation (15), subjected to Equations (6), (7) (replacing Ú by <Ú>) and (16) has also been solved numerically by the finite volume method employing a variant of the computer program used for the 3-D distributed model. At this point, it is worth mentioning that Hsu (1971) solved the 2-D problem numerically and presented some asymptotic expressions for the eigenvalues and the coefficients. Also, Ozisik and Sadeghipour (1982) implemented the matched asymptotic expansion technique and presented highly accurate asymptotic expressions for the determination of the eigenvalues and the coefficients needed for the evaluation of the infinite series for the local Nusselt number. Both expressions for the eigenvalues and the coefficients, valid over the entire range of Biot number (0 μ Bi μ 100), turn out to be extremely intricate for purposes of numerical evaluation. Alternatively, to alleviate these arduous evaluations tabulated the first 12 eigenvalues and coefficients for a selected number of Bi = 0, 0.1, 1, 10 and 100 were presented in Hsu (1971) and Ozisit and Sadeghipour (1982)..

For a more general situation formed by simultaneous development of laminar velocity and temperature, no exact analytic seems to be possible. Owing to this, McKillop *et al.* (1971) resorted to the finite-difference method, whereas Javeri (1976) employed the Galerkin-Kantorovich variational method. A collection of numerical results were presented graphically for the generalized in-tube Nusselt number changing with two parameters: the Prandtl number and the Biot number.

1-D lumped models

a) Variable internal convective coefficient: $h_i(z)$

The objective of this subsection is to transform the 2-D distributed/lumped hybrid model, Equation (15), along with the radial boundary conditions, Equations (7) and (16), into a simpler 1-D lumped model.

First, the concept of the mean-bulk temperature in Equation (2) particularized to laminar motion, corresponds to

$$\langle\Phi\rangle_b(Z) = \frac{\int_\Lambda^{W\langle\Phi\rangle dA}}{\int_\Lambda^{WdA}} = 4\int_0^1 \langle\Phi\rangle(1-\eta^2)\eta \tag{17}$$

Multiplying Equation (15) by gdg and integrating between the proper limits of

zero and one, leads to the equality

$$\int_0^1 (1-\eta^2)\eta\frac{\partial\langle\Phi\rangle}{\partial Z}d\eta = \int_0^1 \frac{\partial}{\partial\eta}\left(\eta\frac{\partial\langle\Phi\rangle}{\partial\eta}\right)d\eta \tag{18}$$

Here again, invoking Leibniz rule (Courant and Hilbert, 1953), the left hand side of this equation is reordered to permit the derivative to occur first. Hence, the end result is

$$4\frac{\partial}{\partial Z}\left(\int_0^1 \langle\Phi\rangle(1-\eta^2) \quad \eta \quad d\eta\right) = 4\int_0^1 \frac{\partial}{\partial\eta}\left(\eta\frac{\partial\langle\Phi\rangle}{\partial\eta}\right)d\eta \tag{19}$$

because the upper and lower limits of the integral are numbers. It may be realized in the LHS of Equation (19) that four multiplied by the term to be differentiated inside the parenthesis is precisely the definition of the dimensionless mean-bulk temperature in Equation (17). Thereby, integration of the RHS of Equation (19) can be completed immediately, giving

$$\frac{\partial\langle\Phi\rangle_b}{\partial Z} = 4\left(\eta\frac{\partial\langle\Phi\rangle}{\partial\eta}\right)_{\eta=1} - 4\left(\eta\frac{\partial\langle\Phi\rangle}{\partial\eta}\right)_{\eta=0} \tag{20}$$

Now, making use of the two radial boundary conditions, Equations (7) (rewritten in terms of <Ú>) and (16), Equation (20) becomes

$$\frac{d\langle\Phi\rangle_b}{dZ} - 4\,Bi\,(1- < \Phi >_{wall}) \tag{21}$$

Unequivocally, the preceding relation necessitates further input from the physics of the problem. It is evident that relevant information about radial heat conduction embedded in the first and second order radial derivatives of Equation (15) has been lost in the process of degrading the 3-D energy equation into a 2-D energy equation. Because the integration in Equation (15) has been performed over the radial coordinate, g, then both the dimensionless mean bulk temperature, $<Ú>_b$, and the dimensionless surface temperature, $<Ú>_{wall}$, in Equation (21) depend solely on the dimensionless axial coordinate, Z. Consequently, to carry out the integration in Equation (21) a relationship between $<Ú>_b$ and $<Ú>_{wall}$, must be established.

For thin-walled tubes, the local, overall heat transfer coefficient, U(z), is basically a harmonic mean of the local internal convective coefficient, $h_i(z)$ and the angular-mean external convective coefficient, h_e,

$$\frac{1}{U(z)} = \frac{1}{H_i(z)} + \frac{1}{\bar{h}_e} \tag{22}$$

To comply with Thermodynamics, it is mandatory that the functions h_i (z) and $\bar{h}_e$ in Equation (22) be associated with an isothermal wall temperature, T_w. For

the former, Churchill and Ozoe (1973) have recommended the correlation equation (A-1) for Nu_i (Z), and for the latter, a group of appropriate spatial-mean Biot numbers, $\overline{Bi}$, has been listed in Appendix B. Actually, Nu_i (Z) exhibits a monotonic decreasing variation with the axial coordinate Z, and renders a position-dependent Nu_{eq} (Z). On the other hand, $\overline{Bi}$, is position-independent.

To remedy for the above deficiency, $\bar{h}_e(<T>_w - T_{\check{s}})$ needs to be replaced by its generalized form $\bar{U}(<T>_b - T_{\check{s}})$. The dimensionless equivalence of this step is analogous to the substitution of $2Bi<\acute{U}>_{wall})$ by $Nu_{eq}(Z)<\acute{U}>_b)$ in Equation (21) where the $Nu_{eq}(Z)$ is defined by

$$\frac{1}{Nu_{eq}(Z)} = \frac{1}{Nu_i(Z)} + \frac{1}{2\overline{Bi}} \tag{23}$$

The explanation in the preceding paragraph insures that the lumped energy equation (16) can be reformulated as an ordinary differential equation of first order as follows

$$\frac{d\langle\Phi\rangle_b}{dZ} = 2[Nu_{eq}(Z)]\ (1 - \langle\Phi\rangle_b), \quad \langle\Phi\rangle_b(0) = 1 \tag{24}$$

Evidently, the highly nonseparable character of Equation (24) necessitates the use of a numerical integration scheme, such as the fourth-order Runge-Kutta algorithm. Certainly, these marching calculations have to be carried out on a personal computer.

b) Axial-mean internal convective coefficient: $\bar{h}_i$.

A further simplification of the 1-D lumped model has been pursued here. The distribution of the local Nusselt number, Nu_i (Z) may be integrated between Z = 0 and Z = L′ to furnish the axial-mean distribution $\overline{Nu}_i(L')$:

$$\overline{Nu}_i(L') = \frac{1}{L'}\int_o^{L'} Nu_i(Z)dZ \tag{25}$$

This step leads to an axial-mean equivalent Nusselt number, $\overline{Nu}_{eq}(L')$

$$\frac{1}{\overline{Nu}_{eq}(L')} = \frac{1}{\overline{Nu}_i(L')} + \frac{1}{2\overline{Bi}} \tag{26}$$

where $L' = L/RRe_iPr_i$ denotes a predetermined dimensionless axial station. In Equation (26), $\overline{Nu}_i(L')$ may be computed from the compact correlation equation (A-2) due to Hausen (1943). Additionally, the set of appropriate spatial-mean Biot number, $\overline{Bi}$ may be found in the Appendix B. At this point, noticing that $\overline{Nu}_{eq}$ is simply a number the ordinary differential equation of first order, Equation (24), transforms into

$$\frac{d\langle\Phi\rangle_b}{dZ} = 2[\overline{Nu}_{eq}(L')]\ (1 - \langle\Phi\rangle_b), \quad \langle\Phi\rangle_b(0) = 1 \tag{27}$$

The analytical solution of this separable equation is readily given by

$$\langle\Phi\rangle_b(L') = 1 - \exp\{[-2\overline{Nu}_{eq}(L')]\ \cdot\ L'\} \tag{28}$$

Suffices to say that the numerical evaluation of Equation (28) is straightforward.

Validation of the 1-D lumped model is mandatory and this issue have been addressed in this sub-section. Consideration is given to an extreme condition accounting for a laminar flow in a tube which is subjected to a vigorous heat rejection caused by a normal forced convection flow of external air. For a limiting condition involving a very large external convective coefficient, $\bar{h}_e$ – > š, the external convective resistance vanishes in Equation (26). This extreme cooling is manifested by the presence of a dominant resistance, i.e., the internal convective resistance ensuring the simplification of $\overline{Nu}_{eq}$ into $\overline{Nu}_i$ in Equation (26). On introducing $\overline{Nu}_i$ into Equation (28) the dimensionless mean bulk temperatures, $<\acute{U}>_b$, linked to a limiting isothermal wall condition should be recovered. As a corollary of this, the dimensionless wall temperature, $<\acute{U}>_b$ tends to zero. The set of $<\acute{U}>_b$ predictions supplied by the algebraic solution of the 1-D lumped model compared perfectly with the benchmark $<\acute{U}>_b$ results of the 2-D distributed model with an analytic solution. The latter solution is taken from Table 13 in Shah and London (1978).

In sum, it is important to realize that the first 1-D lumped model, based on a function Nu_{eq} (Z) required numerical integration with a Runge-Kutta algorithm. In contrast, the second 1-D lumped model is controlled by merely a number $\overline{Nu}_{eq}$ and the evaluations can be carried out with a calculator. The latter lumped model seems to have an aggregate advantage over the former lumped model because by virtue of Equation (1) an analytical correlation equation for the dimensionless total heat transfer, õ$_t$, may be constructed immediately. That is:

$$\Omega_t = 1 - \exp\{[-2\overline{Nu}_{eq}(L')]\ \cdot\ L'\} \tag{29}$$

At this point, a comment about the modeling of internal turbulent flows is in order. In general, the internal thermal resistance for turbulent flows in externally finned tubes is substantially smaller than that of laminar flows. Therefore, under comparable conditions, the external resistance will play a more decisive role in the former than in the latter. On this basis, it may be expected that external finning will be more effective for turbulent tube flows than for laminar tube flows. The excellent quality of the results for laminar flows lent credibility to the 1-D lumped model with its algebraic solution so that the idea can be extended to turbulent flows without hesitation. Under these circumstances, $\overline{Nu}_i(L'')$ may be computed from the compact correlation equation (A-4) suggested by Stein (1988).

Discussion of results

Owing to an abundance of geometric and thermal parameters, severed by journal space limitations, a full parametric exploration seems to be unrealistic and only representative results have been given here for two selected arrays of plate fins. One array is sparse consisting of N = 4 fins, while the other is dense made of N = 16 fins. Moreover, the same fixed values of the prescribable dimensionless parameters $X_f = 0.05$, $Bi_f = 50$ and $Bi_u = 1$ used in Sparrow and Charmchi (1980) and Moukalled *et al.* (1992) have been chosen throughout the present calculations. For each array, the size of the unfinned segment, X_u, is determined from the peripheral relation $D = N \cdot X_f + N \cdot X_u$. Besides, the values of the spatial-mean Biot numbers, $\overline{Bi}_a$, $\overline{Bi}_g$, and $\overline{Bi}_h$, are evaluated from the formulas (B-1)-(B-3) listed in Table I.

Introducing a dimensionless heat transfer (or heat transfer efficiency), k_t, converts Equation (1) into

$$\Omega_t = \frac{Q_t}{Q_{\max}} = \frac{Q_t}{rh\ c_{p,i}\ (T_0 - T_\infty)} = \langle \Phi \rangle_b (L') \tag{30}$$

in which $\acute{U}_b(L')$ is the mean bulk temperature at a position, L′, both dimensionless quantities. Therefore, this equality implies that knowledge of $\acute{U}_b$ at any predetermined downstream station, L′, is synonymous with the total heat transfer, Q_t, up to that station. In passing, it should be mentioned that the thermodynamic procedure avoids the calculation of an additional thermal quantity, the local finned-tube Nusselt number Nu_z, which among other things depends on the characteristics of the fin array and the type of cooling.

For purposes of comparison, the mean bulk temperatures, $\acute{U}_b$ (or their equivalent total heat transfer rates, $\tilde{o}_t$), supplied by the complete, 3-D distributed model owing to an angular variation of the Biot number, Bi(h), have been regarded as the baseline solution. Accordingly, the exact numbers for $\tilde{o}_t$ are plotted with a solid line in Figures 2 and 3 for N = 4 and a four-fold increment in the number of fins, N = 16. As may be anticipated, under comparable circumstances and identical values of X_f, X_u, Bi_f, and Bi_u, the total heat removal, $\tilde{o}_t$, in a tube of finite length L′ varies proportionally with the number of fins N in the array.

Without loss of generality, we should expect that the curves for the total heat transfer, $\tilde{o}_t$, based on the 3-D model, must lie between those curves plotted with the approximate 2-D and 1-D total heat transfer calculated with the appropriate spatial means of the Biot number. The format adopted in each family of curves

Table I. Geometric and thermal characteristics of two fin arrays

N	Xf	Bif	Xu	Biu	Bia	Big	Bih
4	0.05	50	0.735	1	4.12	1.28	1.07
16	0.05	50	0.146	1	13.50	2.71	1.33

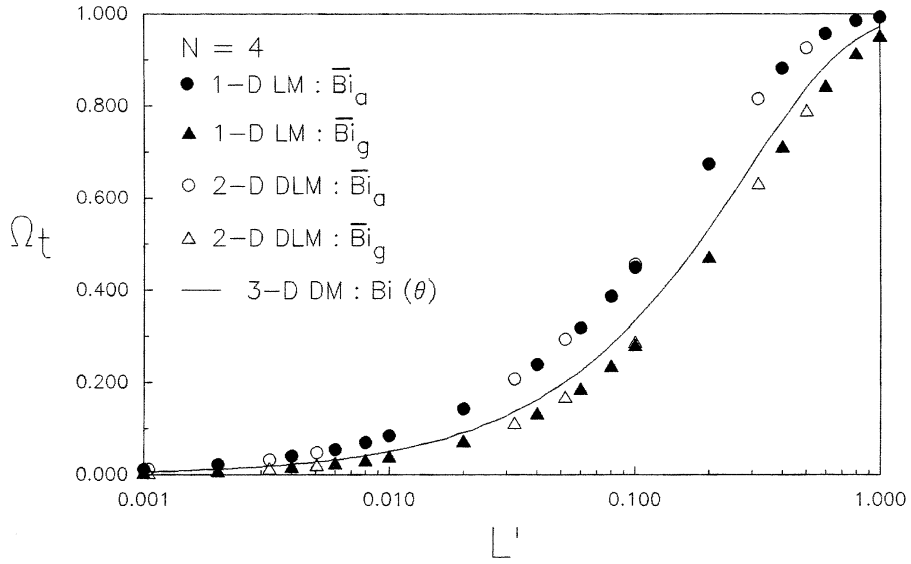

Figure 2.
Axial variation of the total heat transfer for N = 4 computed with the 3-D, 2-D and 1-D models

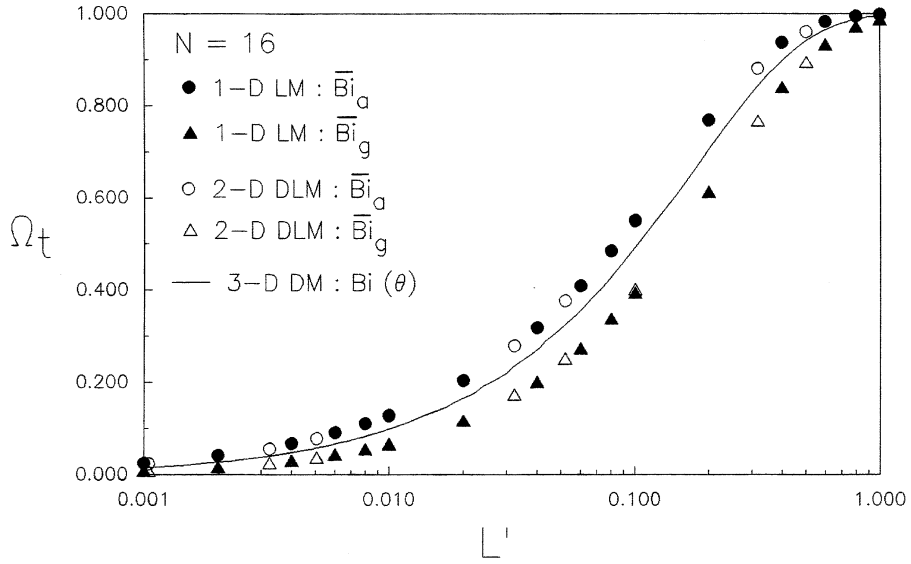

Figure 3.
Axial variation of the total heat transfer for N = 16 computed with the 3-D, 2-D and 1-D models

is as follows: the upper curve is associated with the arithmetic spatial mean, $\overline{Bi}_a$, the middle curve represents the harmonic weighted-spatial mean, $\overline{Bi}_g$, and the lower curve pertains to the geometric spatial mean of Bi, $\overline{Bi}_h$.

Aside from the fact that $\overline{Bi}_a$ constitutes a strong upper bound, able to estimate the maximum heat liberation of the externally finned tube, say $\tilde{o}_{t,max}$, a question that needs to be addressed is whether $\overline{Bi}_g$ or $\overline{Bi}_h$ provide a strong or a weak lower bound. Undoubtedly, one of the two will be able to estimate the minimum heat liberation of the externally, finned tube, $\tilde{o}_{t,min}$, in a better way.

The heat transfer results supplied by the 2-D model involving the harmonic-spatial-mean, $\overline{Bi}_h$, are not plotted in the figures in order to preserve clarity. The rationale behind this decision is that, when compared with the real heat transfer based on the 3-D model, the $\tilde{o}_t$-curves for $\overline{Bi}_h$ consistently fell below those for the geometric-spatial-mean, $\overline{Bi}_g$ (in conformity with the inequalities (B-4)). This behavior suggested that $\overline{Bi}_h$ was a weaker lower bound and because of this attribute can be discarded. In contrast, $\overline{Bi}_g$, being a stronger lower bound, was indeed a better statistical estimate. This sequential pattern is in perfect accordance with the inequalities (B-4) derived from statistical analysis.

Comparison between the total heat transfer delivered by the 2-D and the 1-D lumped models

To facilitate the comparison between the 2-D and 1-D models in Figures 2 and 3, the total heat transfer based on $\overline{Bi}_a$ are portrayed by circles, while those for $\overline{Bi}_g$ are illustrated by triangles. The curves that are situated in the upper part of each figure were generated with the 1-D lumped model involving an arithmetic spatial-mean, $\overline{Bi}_a$, whereas those in the lower part of the figures are linked to the 1-D lumped model involving a geometric spatial-mean, $\overline{Bi}_g$. For all the fin arrays examined ($4 \mu N \mu 16$), the $\tilde{o}_t$-curves connected to the 1-D lumped model fall directly on top of the $\tilde{o}_t$-curves related to the 2-D distributed/lumped hybrid model with the same means. This concordance is a strong affirmation of the forgiving nature of the angular dependency of the external convective coefficients, $h_e(h)$, in favor of the selected spatial means. It turns out that the $h_e(h)$-variation is conveniently embedded into the two reliable spatial means, $\bar{h}_a$ and $\bar{h}_g$, respectively in the 2-D distributed/lumped hybrid model as well as in the 1-D lumped model. Therefore, in view of this systematic overlapping of the curves, attention has been focused on the one-to-one comparison between the 3-D distributed and the 1-D lumped models in the following sub-section.

Comparison between the total heat transfer furnished by the 3-D and the 1-D lumped models

First, the heat transfer, $\tilde{o}_t$, computed with the 3-D model and its variable external convective coefficient, $h_e(h)$, has been compared against the approximate heat transfer supplied by the 1-D model based on the two candidate spatial means, $\overline{Bi}_a$ and $\overline{Bi}_g$, in Figures 4 and 5. Here, it may be observed that for a sparse array, $N = 4$, the two types of 1-D solutions embrace the 3-D solution perfectly. In addition, the approximate $\tilde{o}_t$-curve supplied by the 1-D model with a geometric spatial mean, $\overline{Bi}_g$, is moderately lower than the accurate heat transfer curve based on the 3-D model. It may be inferred that the curve of the 1-D model is shifted upwards, providing a qualitative lower-bounded, statistical estimate. Here, the disparity between the approximate heat transfer of the 1-D model with an arithmetic spatial mean, $\overline{Bi}_a$, and the precise heat transfer of the 3-D model is small. As the number of fins in the array was increased gradually to 8, and later to 12, an approximate symmetrical behavior

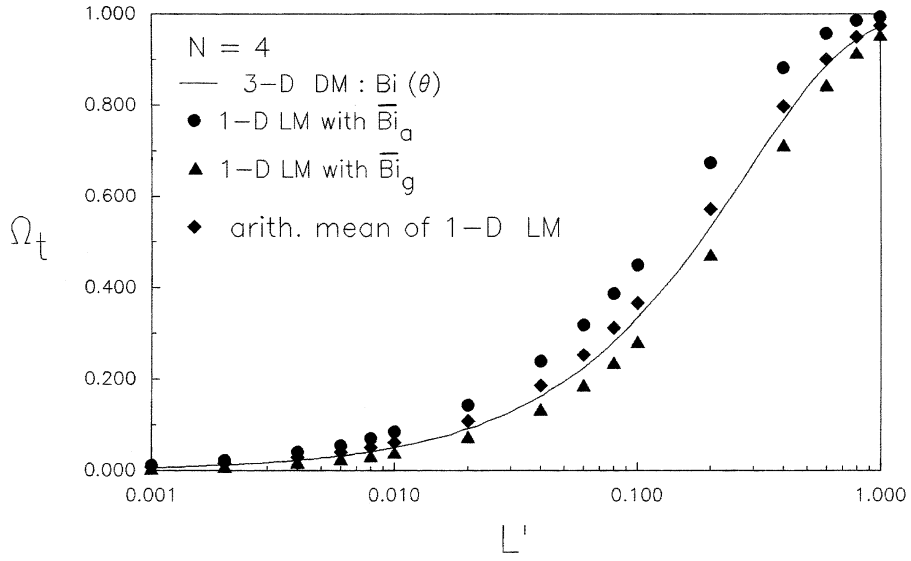

Figure 4.
Comparison of the axial variation of the total heat transfer for N = 4 obtained by the exact 3-D distributed model and the arithmetic mean of the two bounding 1-D lumped models

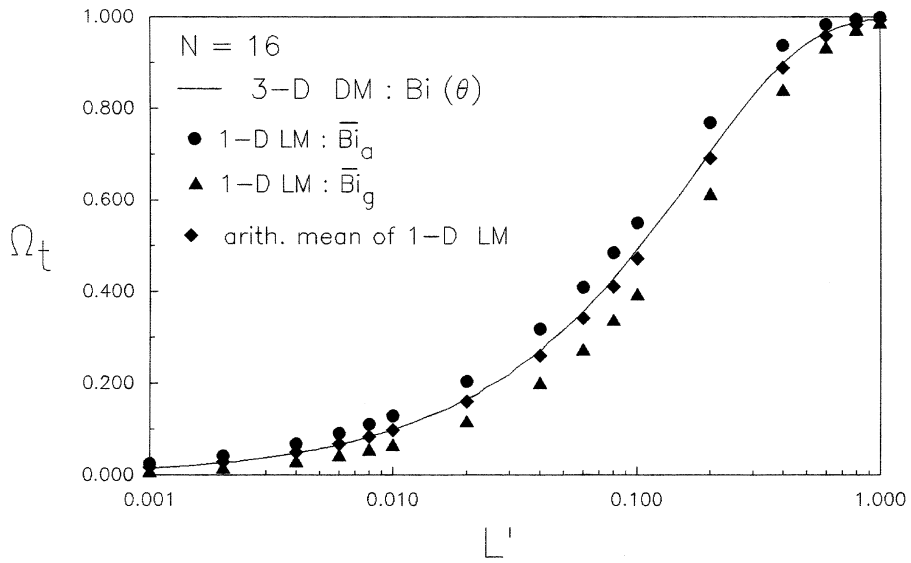

Figure 5.
Comparison of the axial variation of the total heat transfer for N = 16 obtained by the exact 3-D distributed model and the arithmetic mean of the two bounding 1-D lumped models (DM: distributed model and LM: lumped model)

was noticed and the $\tilde{o}_t$-curves based on the 3-D model were equidistant from the two simplified 1-D bounding curves based on $\overline{Bi}_a$ and $\overline{Bi}_g$ for brevity. Contrary to the case for N = 4, the opposite pattern is in evidence for a dense array of N = 16 fins. This tendency demonstrates that the heat transfer curve of the 1-D model is shifted downwards, supplying a qualitative upper-bounded statistical estimate. Besides, it may be observed that the discrepancy between the approximate heat transfer of the 1-D model with an arithmetic spatial-mean, $\overline{Bi}_a$, and the precise heat transfer of the 3-D accurate model is again small. The

features displayed in Figures 4 and 5 are worthy of note because they put in unequivocal evidence an intrinsic sweeping behavior of the 1-D $\tilde{o}_t$-curves that do respond to the number of fins in the array.

Taking advantage of the fact that the two types of 1-D algebraic solutions bracketed the accurate 3-D finite-difference solution, a new predictive method may be proposed. It involves the straightforward use of an arithmetic mean of the two 1-D bounding solutions of the heat transfer accounting for $\overline{\mathrm{Bi}}_a$ and $\overline{\mathrm{Bi}}_g$, respectively. This leads to the simple formula

$$\Omega_t = \frac{1}{2}[\Omega_t(\overline{Bi}_a) + \Omega_t(\overline{Bi}_g)] \tag{31}$$

whose repercussions have been explored in this subsection. It is expected that the new approach can match the complete 3-D solution in a better way and provide the best estimation of $\tilde{o}_t$. To accomplish this, the arithmetic spatial means for the heat transfer have been computed varying the dimensionless length, L′, for N = 4 and 16 fins and are plotted in Figures 4 and 5 as well. Here, from an overall appraisal of these two figures, it is seen that none of the new 1-D heat transfer predictions represented by filled rhombics are very far from those given by the precise 3-D heat transfer results.

A qualitative comparison of the heat transfer deviations at several axial positions has also been carried out using the two diametrically opposed methods. First, for N = 4, the $\tilde{o}_t$-deviations are insignificant always within a margin of 0.04 units in the entire heat exchange region. Conversely, for N = 16, the $\tilde{o}_t$-deviations are practically nullified, and never exceeded 0.01 units in the entire heat exchange region.

As a final matter, attention has been turned to the thermal design of finned tubes for heat exchange devices. The simplistic 1-D temperature distributions (synonymous with the total heat transfer) can be computed by hand because the operations involve simple algebra. Thus, these bounding results can be used later to calculate the arithmetic mean of the two 1-D heat transfer solutions and, if necessary, may be fitted with available curve fit software. Consequently, the resulting correlation equation is of the type

$$\Omega_t^{-1} = a + \frac{b}{L'} \tag{32}$$

where a and b are constants. This equation may be valuable to thermal design engineers who need to expedite the calculations. Otherwise, precise calculations may necessitate the use of the 3-D numerically-determined results generated by the computer and a companion set of graphs.

In sum, the central implication of the approximate bounding results, via a plain 1-D lumped model, is that it may safely replace the numerical results provided by the 3-D distributed model for this kind of finned-tube, forced convection problem.

Conclusions

It may be concluded that a 3-D partial differential energy equation with variable coefficients and a boundary condition of third kind possessing a marked periodicity may be safely converted into a simple 1-D ordinary differential equation of first order. The bounding treatment of the dominant boundary condition was successfully handled with appropriate statistical spatial means. Statistical spatial means seem to provide a very useful tool in a variety of situations in engineering analysis, and their applications are quite underdeveloped. We hope that this introduction to the topic of statistical heat transfer in finned tubes has stimulated the reader's interest.

References

Bergles, A.E. (1998), "Techniques to enhance heat transfer", in Rohsenow, W.M. *et al.* (Eds), Chapter 11, *Handbook of Heat Transfer*, 3rd ed, McGraw-Hill, New York, NY.

Churchill, S.W. and Ozoe, H. (1973), "Correlations for laminar forced convection in flow over an isothermal flat plate and in developing and fully developed flow in an isothermal tube", *ASME J. Heat Transfer*, Vol. 95, pp. 416-23.

Courant, R. and Hilbert, D. (1953), *Methods of Mathematical Physics*, Interscience, New York, NY.

Gnielinski, V. (1976), "New equations for heat and mass transfer in pipe and channel flow", *Intern. Chemical Engng.*, Vol. 16, pp. 359-67.

Hardy, G.H., Littlewood, J.E. and Polya, G. (1967), *Inequalities*, Cambridge Press, London.

Hausen, H. (1943), "Darstellung des Warmeuberganges in Rohren durch verallgemeinerte Potenzbeziehungen", *Z. VDI Beih. Verfahrens-tech*, No. 4, pp. 91-102.

Hsu, C.J. (1971), "Laminar flow heat transfer in circular or parallel-plate channels with internal heat generation and the boundary condition of the third kind", *J. Chinese Institute Chem. Engng.*, Vol. 2, pp. 85-100.

Jakob, M. (1949), *Heat Transfer*, Vol. I, Mc-Graw Hill, New York, NY.

Javeri, V. (1976), "Simultaneous development of the laminar velocity and temperature fields in circular duct for the temperature boundary condition of the third kind", *Intern. J. Heat Mass Transfer*, Vol. 19, pp. 943-9.

Kays, W.M. and Crawford, M.E. (1993), *Convective Heat and Mass Transfer*, 3rd ed., McGraw-Hill, New York, NY.

Legkiy, V.M., Pavlenko, V.P., Makarov, A.S. and Zheludov, Y.A. (1974), "Investigation of local heat transfer in a tube with annular fins in transverse air flow", *Heat Transfer-Soviet Research*, Vol. 6, pp. 101-7.

McKillop, A.A., Harper, J.C. and Bader, H.J. (1971), "Heat transfer in entrance region flow with external resistance", *Intern. J. Heat Mass Transfer*, Vol. 14, pp. 863-6.

Mills, A.F. (1992), *Heat Transfer*, Irwin, Boston, MA.

Moukalled, F., Kasamani, J. and Acharya, S. (1992), "Turbulent convection heat transfer in externally finned pipes", *Numer. Heat Transfer, Part A*, Vol. 21, pp. 401-21.

Ozisik, M.N. and Sadeghipour, M.S. (1982), "Analytic solution for the eigenvalues and eigencoefficients of the Graetz problem with third kind boundary condition", *Intern. J. Heat Mass Transfer*, Vol. 25, pp. 736-9.

Patankar, S.V. (1980), *Numerical Heat and Fluid Flow*, Hemisphere, New York, NY.

Petukhov, B.S. (1970), "Heat transfer and friction in turbulent pipe flow with variable physical properties", *Advances in Heat Transfer*, Vol. 6, Academic Press, New York, NY, pp. 504-64.

Schmidt, Th.E. (1963), "Der Wärmeübergang an rippenrohren und die Berechnung von rohrbündel", *Wärmeaustauschern Kältetechnik*, Vol. 15 No. 12, pp. 370-8.

Seider, E.N. and Tate, G.E. (1936), "Heat transfer and pressure drop of liquids in tubes", *Industrial Engng. Chemistry*, Vol. 28, pp. 1429-35.

Settari, A. and Aziz, K. (1973), "A generalization of the additive correction methods for the iterative solution of matrix equations", *SIAM J. Numer. Analysis*, Vol. 10, pp. 506-21.

Shah, R.K. and London, A. (1978), *Laminar Forced Convection in Ducts*, Academic, New York, NY.

Sparrow, E.M. and Charmchi, M. (1980), "Laminar heat transfer in an externally finned circular tube", *ASME J. Heat Transfer*, Vol. 102, pp. 605-11.

Stein, W.A. (1988), "Eine neue Gleichung für den Wärme-und den Stoffübergang in durchströmten Rohren (Teil 1)", *Forschung aim Ingenieurwesen*, Vol. 54, pp. 117-22.

Webb, R.L. (1994), *Principles of Enhanced Heat Transfer*, Wiley, New York, NY.

Appendix A. Theoretical distributions of the axial-mean Nusselt numbers which are required for the models

1. In-tube flows with prescribed temperature at the wall

1a. Fully developed laminar velocity for water and oil. For laminar flow ($Re_i < 2000$) and developing temperature, the local Nusselt number, $Nu_i(Z)$, may be computed from the correlation equation developed by Churchill and Ozoe (1973):

$$Nu_i(Z) = 5.357\left[1 + \left(\frac{61.752}{Z}\right)^{-8/9}\right]^{3/8} - 1.7 \tag{A1}$$

The axial-mean Nusselt number, $\overline{Nu}_i(L)$, may be obtained from the correlation equation proposed by Hausen (1943):

$$\overline{Nu}_i(L) = 3.657 + \frac{0.067\left(\frac{D_i Re_i Pr_i}{L}\right)}{1 = 0.04\left(\frac{D_i re_i Pr_i}{L}\right)^{2/3}} \tag{A2}$$

1b) Developing laminar velocity for any fluid. For this general flow condition (Re_i μ 2000), Kays and Crawford (1993) have recommended that for internal fluids with Prandtl numbers greater than five (e.g. water and oil), the laminar velocity profiles develop so much faster than the temperature profile that the assumption of fully developed laminar velocity at the tube entrance seems to be reasonable and thereby introduces little error. Hence, Equation (A1) and (A2) apply equally well for situations of simultaneous development of velocity and temperature for water and oil.

For the specific case of air, the simultaneous laminar flow and temperature may be modelled by the correlation equation for the axial-mean Nusselt number, $\overline{Nu}_i(\bar{L})$ recommended by Stein (1988):

$$\overline{Nu}_i(L) = \left[\left(\frac{3.66\ Pr_i + 0.576}{Pr_i + 0.1}\right)^3 + (1.62)^3\left(\frac{D_i Re_i Pr_i}{L}\right) + \frac{(0.664)^3\ Pr_i\left(\frac{D_i Re_i}{L}\right)^{3/2}}{1 + \frac{0.204}{Pr_i^{1/2}}}\right]^{1/3} \tag{A3}$$

1c) Fully developed turbulent velocity of any fluid. For fully developed turbulent velocity ($2000 < Re_i < 10^6$) and developing temperature, the axial-mean Nusselt number, $\overline{Nu}_i$, may be determined from the two correlation equations constructed by Gnielinski (1976):

$$\overline{Nu}_i = 0.0214\ (Re_i^{0.8} - 100)\ Pr_i^{0.4}\left[1 + \left(\frac{D}{L}\right)^{2/3}\right] \tag{A4a}$$

for gases ($0.6 < Pr < 1.5$) and

$$\overline{Nu}_i = 0.012\ (Re_i^{0.87} - 280)\ Pr_i^{0.4}\left[1 + \left(\frac{D}{L}\right)^{2/3}\right] \tag{A4b}$$

for liquids ($1.5 < Pr < 500$), respectively.

1d) Influence of temperature-dependent properties. There are simple correction factors used in engineering practice that adjust the constant-property correlation equations to accommodate the effects of property variation of fluids.

For liquids, the correction factor is

$$\frac{\overline{Nu}_{i,vp}}{\overline{Nu}_i} = \left(\frac{\mu_b}{\mu_w}\right)^n \tag{A5}$$

where $\grave{I}_b$ and $\grave{I}_w$ are evaluated at their respective temperatures T_b and T_w.

For gases, the correction factor is

$$\frac{\overline{Nu}_{i,vp}}{\overline{Nu}_i} = \left(\frac{T_b}{T_w}\right)^n \tag{A6}$$

where T_b and T_w are the absolute mean bulk and wall temperature, respectively. In both equations, $\overline{Nu}_{i,vp}$ designate variable properties, whereas $\overline{Nu}_i$ represent constant properties. Numerical values of n are listed in Table AI.

Appendix B. Statistical analysis of the spatial means of the angular variation of the Biot numbers

The local external convective coefficient, $h_e(h)$, shown in Figure 1b may be modeled as a periodic variation of low values of the external convective coefficient, h_u, for the unfinned portion, x_u, and high values of the external convective coefficient, h_f, for the finned portion, x_f, respectively. The resulting strong discontinuous change may be recast in dimensionless form as two different Biot numbers: Bi_u and Bi_f belonging to their respective unfinned and finned segments, X_u and X_f.

For the sake of generality, let us assume the existence of a uniform distribution of $h_e(h)$ in an unfinned- finned interval between $X = 0$ and $X = X_u + X_f$, where the coordinate X is measured along the tube circumference. Statistical Theory (see Hardy *et al.* (1967)) classifies three different spatial-means. In the context of this study, the three notable spatial-mean Biot numbers, $\overline{Bi}$, are:

Type of flow	Fluid	Condition	n	Reference
Laminar	Liquid	Cooling/heating	0.14	Seider and Tate (1936)
Laminar	Gas	Cooling/heating	0	Kays and Crawford (1993)
Turbulent	Liquid	Cooling	0.25	Petukhov (1970)
Turbulent	Liquid	Heating	0.11	Petukhov (1970)
Turbulent	Gas	Cooling	0	Kays and Crawford (1993)
Turbulent	Gas	Heating	0.5	Kays and Crawford (1993)

Table AI. Values of the exponent n in equations (A5) and (A6)

a) the arithmetic spatial-mean:

$$\overline{Bi}_a = \frac{X_u Bi_u + X_f Bi_f}{X_u + X_f} \tag{B1}$$

b) the geometric spatial-mean:

$$\overline{Bi}_g = \left(Bi_u^{X_u} \, Bi_f^{X_f} \right)^{\frac{1}{X_u + X_f}} \tag{B2}$$

and

c) the harmonic spatial-mean:

$$\overline{Bi}_h = \left[\frac{1}{X_u + X_f} \left(\frac{X_u}{Bi_u} + \frac{X_f}{Bi_f} \right) \right]^{-1} \tag{B3}$$

respectively.

Further, it can also be demonstrated that these three spatial means are quantitatively related by the inequalities

$$\overline{Bi}_a < \overline{Bi}_g < \overline{Bi}_h \tag{B4}$$

In essence, the goodness of the spatial-mean Biot numbers may serve as a criterion for the correctness of the bounding procedure for the real distributions of the mean bulk temperature and the total heat transfer during the course of the adoption of a 2-D distributed/lumped hybrid model and a 1-D lumped model.